CFD simulations of large scale LH2 dispersion in open environment

S.G. Giannissi[1,*], A.G. Venetsanos[1], E. Vyazmina[2], S. Jallais[2], S. Coldrick[3], K. Lyons[3]

[1] Environmental Research Laboratory, National Center for Scientific Research Demokritos, Aghia Paraskevi, Athens, 15341, Greece, sgiannissi@ipta.demokritos.gr

[2] Centre de Recherche Paris-Saclay, Air Liquide Research & Development, 1, chemin de la Porte des Loges, Les Loges-en-Josas – BP 126, 78354 Jouy-en-Josas, France

[3] Health and Safety Executive, Harpur Hill, Buxton, SK17 9JN, UK

ABSTRACT

An inter-comparison among partners' CFD simulations has been carried out within the EU-funded project, PRESLHY, to investigate the dispersion of the mixture cloud formed from large scale liquid hydrogen release. Rainout experiments performed by Health and Safety Executive (HSE) have been chosen for the work. From the HSE experimental series trial-11 was selected for simulation due to its conditions where only liquid flow at the nozzle was achieved. During trial-11 liquid hydrogen is spilled horizontally 0.5 m above a concrete pad from a 5 barg tank pressure through a 12 mm (1/2 inch) nozzle. The dispersion takes place outdoors, and thus it is imposed to variant wind conditions. Comparison of the CFD results with the measurements at several sensors is presented and useful conclusions are drawn.

Keywords: hydrogen, dispersion, CFD, liquid release, safety

1.0 INTRODUCTION

The European Green Deal that was signed in 2019 sets policy initiatives with the aim of making Europe climate neutral in 2050. Among the goals of the Green Deal is the reduction of greenhouse gases by 50-55% until 2030 and no net emissions by 2050. Hydrogen can play a vital role in fulfilling the goals of this deal if used in transport sector due to its carbon zero-emissions. For that reason European Commission announced investments of 180 to 470 billions in hydrogen technologies.

For the massive use of hydrogen as fuel in heavy-duty vehicles, such as trucks, buses, trains and especially ships it is critical to obtain the required knowledge for its safe use and to develop relevant regulations, standards and codes based on state-of the-art. PRESLHY project [1] is an EU-funded project with the aim to perform pre-normative research for the safer use of liquid hydrogen (LH2), as LH2 is considered the most appropriate candidate for heavy vehicles. PRESLHY project covers a wide range of safety aspects related to LH2, such as release and dispersion, pool formation, ignition, combustion, etc.

Within PRESLHY an inter-comparison of CFD simulations of LH2 dispersion in open environment was carried out by two partners, Air Liquide (AL) and National Center for Scientific Research "Demokritos" (NCSRD). The simulations were based on LH2 rainout experiments conducted by Health and Safety Executive (HSE) in their experimental site in Buxton [2], [3]. A series of 25 trials were carried out using different release diameters, storage pressure, release heights and directions. All trials took place outdoors and thus were exposed to naturally varying wind. Trial 11 was selected for simulation, because the experimental data indicated that the flow at the nozzle was most likely all liquid. Therefore and since it was unable to measure the exact vapour quality at the nozzle, this trial was chosen so as not to introduce uncertainties involving the conditions at the nozzle. During the experiment LH2 was released through a 12 mm nozzle from a height of 0.5 m from the ground. The gauge pressure at the storage tank was 5 bar.

The inter-comparison among the partner's simulations and the experimental results is presented here. Due to wind intermittency consistent comparison using the time series is not possible. Thus, it is considered that the measured maximum concentration in each sensor along release centerline is achieved when the wind is aligned with the release. This peak value is compared with the predicted

steady state concentration at the sensors located on the jet centerline plane. Similarly, we compare the measured minimum temperature with the respective predicted one.

2.0 HSE EXPERIMENTAL DESCRIPTION

HSE experiments involve liquid hydrogen release and dispersion in open environment [2]. The main objective of the HSE experimental series was to investigate LH2 rainout when LH_2 is released from elevated positions and to develop a database for codes' validation in LH2 release and dispersion. A series of 25 unignited LH2 releases was carried out through 6 mm, 12 mm, and 25.4 mm nozzles from tank pressure of 1 bar or 5 barg and release heights of 0.5 m or 1.5 m. Different release directions (horizontal and vertical downwards) were examined.

Both concentration and temperature were measured. Parameters such as pressure, mass flow rate and temperature were also measured in the pipework, in order to provide an insight on hydrogen exit conditions. Videos during the release duration showing the cloud dispersion are also available. The experiments were carried out using the LH2 release facility, located on a 32 m diameter concrete pad at the Frith Valley site at the HSE Science and Research Centre in Buxton.

For this work, trial 11 was selected since it was a test that only liquid flow was established at the hydrogen exit. The release was horizontal from 0.5 m height at 5 barg and through 12 mm nozzle. Figure 1 shows the experimental mass flow rate time series and the flow rate that was set as hydrogen inlet condition in ADREA-HF simulations (see Section 3.2). The steady state mass flow rate was 265 g/s. After 200 sec there is a short departure from stable flow most likely due to some detachment of a pocket of vapor somewhere in the delivery system. This would expose the flow to a relatively warm section of pipe, which would result in enhanced heat transfer that disturbed the flow.

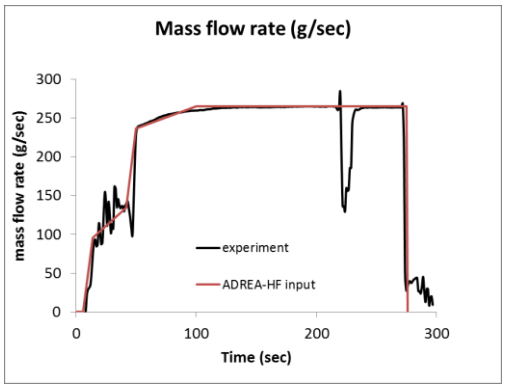

Figure 1. The measured mass flow rate and the rate that was set as input in ADREA-HF simulations.

Wind was blowing with average speed equal to 2.7 m/s at 1.5 m height in the near-field and 2.9 m/s at 3 m height based on far-field measurements. The average near-field wind direction was 300 degrees and the average far-field 276 degrees with the jet release centreline direction to be in 75 degrees from north, i.e. a wind direction of 255 degrees would be considered co-flow.

Several sensors and thermocouples have been placed along the release centreline and in lateral positions. The sensors are distinguished in near–field and far-field measurements stations. The near field sensors measure until 6 m downwind the nozzle. The far-field sensors were placed along two arcs, one with radius 10 m from the nozzle and the other with radius 14 m from the nozzle.

3.0 CFD MODELLING

Two partners, AL and NCSRD, with two different codes, ADREA-HF and FLACS, respectively, have simulated the experiment. Next, a brief description of the modeling strategy of each partner is presented.

3.1 AL

Air Liquide used the commercial CFD code FLACS v20.1 [4] developed by Gexcon AS. The code is dedicated to modeling of dispersion and explosion accidents at an industrial scale. The code is able to correctly handle cases with geometries from $1m^3$ up to the size of an offshore platform or a huge industrial plant. FLACS can solve both compressible and incompressible Navier-Stokes equations on 3D Cartesian grid using finite volume approach. No symmetry is assumed in the current simulations. FLACS solves conservation equations for mixture mass, momentum, enthalpy, and mass fraction of hydrogen, which are closed by the ideal gas law. It uses the Reynolds-averaged Navier-Stokes (RANS) approach in particular a standard k-eps model with a modification[4], [5]. Turbulence model is coupled with a sub-grid model to take into account small objects that cannot be resolved on the computational grid. In the current modeling approach, all obstacles (ground) were represented on the grid; hence, there was no influence of the sub-grid model on the simulation results.

Second-order ‘‘kappa’’ scheme (hybrid scheme with weighting between 2^{nd} order upwind and 2^{nd} order central differences, with limiters for some equations) was applied for convection term, whereas second-order was used for the diffusion term. For the integration in time, the first order backward Euler scheme was employed. FLACS guidelines recommend to use CFLC=10 (based on speed of sound) and CFLV =1 (based on flow velocity) for dispersion modelling, these guidelines were followed in the current study. Transient simulations were run until reaching the steady state (approximately after 100-200 sec). Simulations were also performed with a higher CFLV=5 (CFLC is fixed to 10 in both cases) and the results found to be in close agreement with the ones with the lower CFLV.

The simulation domain was X= [-9.284 m, 20.716 m] in stream wise direction, Y= [-15m, 15m] in cross-stream and Z= [-0.12m, 10m] in the vertical direction. It is assumed that the physical source is located at the point with coordinates [0, 0, 0.5 m]. FLACS user’s guide [4] recommends using one cell for representation of the high velocity release point in the Y and Z, in order the release to be fully integrated into one cell. The second cell to the release point should be of the same size; further, the cell size can be increased. In current simulations the grid was regular in X direction of dx=0.2 m corresponding to 150 number of the control volume in this direction. The base size of the grid in Y direction was 0.2 m, whereas it was refined at the source position up to 0.176 m, the maximum stretching parameter was 1.15 in Y direction; the total number of control volumes is 159. The base size of the grid in Z direction was 0.2 m, whereas it was refined at the source to 0.176 m. The total number of control volumes in Z direction is 52. The total number of control volumes was 1 240 200.

The current version of FLACS is able to model the dispersion of only gaseous phase, no two-phase releases are possible. FLASH utility program [4]-[6] is used for the modeling of the release of liquid hydrogen. The model assumes that a part of the liquefied gas may rain out (in this case the rain out is negligible and this was also observed in the experiments) the rest remains in the jet form as an aerosol or spray and it is gradually evaporated. After the flashing the gas mixes with the ambient air. Dry ambient air was assumed. The utility gives an equivalent source (mass flow rate, diameter, temperature, mass fraction of the released gas and air) and the axial distance at which the whole cloud is evaporated and partially mixed with the ambient dry air. Data from the FLASH utility program are used as the input parameters to the CFD dispersion modeling. Following parameters were used as the input to the FLASH utility: the mass flow rate is 0.265 kg/s; the temperature of liquefied gas at the orifice is -245°C, the ambient temperature is 15.712°C. Table 1 shows the output data for the FLASH utility program, which are used as the input conditions for the hydrogen dispersion.

Table 1. Output data of FLASH utility program.

Axial distance at which the jet is fully evaporated	0.7660031 m
Equivalent jet area	0.0196984 m^2
Equivalent jet mass flow	0.7111812 kg/s
Temperature of the equivalent jet	-253.1362 °C
Equivalence ratio of released gas in entrained jet	20.5324
Mass rate of liquefied gas that rains out and forms a pool	79.5997 10^{-15} (kg/s)

Taking into account the offset of the sensors position and the distance to the equivalent source, the modelled release is located in simulations at the point with coordinates [0.716 m, 0, 0.5 m].

Wind boundary condition is applied at low X boundary; see [4], [7], [8]. In FLACS the Monin-Obukhov length is estimated by using Pasquill classes. Logarithmic profile is applied for the wind velocity. Current simulations were run using following parameters: D-stability class (no thermal stratification of the atmosphere), ground roughness is 0.03m, ambient temperature is 15.7°C and wind velocity is 2.7 m/s at 1.5 m.

3.2 NCSRD

NCSRD used the ADREA-HF CFD code, which is a widely validated code in several applications, including dispersion of liquefied gases [9][10][11][12]. It solves the fully compressible, time-dependent, 3D conservation equations for the mixture mass, momentum and enthalpy along with the mass fraction conservation equations of the components in the mixture. The mass fraction of the most abundant fluid (most commonly air) is not solved and is estimated from the other mass fractions using the constraint that the sum of the mass fraction of all components should be equal to unity. In the present study the humidity was not modeled and the air was modeled as one component (with mass-weighted properties based on its composition in nitrogen and oxygen). No phase change is permitted to air. The governing equations are:

$$\frac{\partial \rho}{\partial t} + \frac{\partial \rho u_i}{\partial x_i} = 0 \tag{1}$$

$$\frac{\partial \rho u_i}{\partial t} + \frac{\partial \rho u_i u_j}{\partial x_j} = -\frac{\partial P}{\partial x_i} + \frac{\partial}{\partial x_j}\left((\mu + \mu_t)\left(\frac{\partial u_i}{\partial x_j} + \frac{\partial u_j}{\partial x_i} \right) \right) + \rho g_i \tag{2}$$

$$\begin{aligned} \frac{\partial \rho h}{\partial t} + \frac{\partial \rho u_i h}{\partial x_i} = \frac{dP}{dt} + \frac{\partial}{\partial x_i}\left((\lambda + \lambda_t)\frac{\partial T}{\partial x_i} \right) \\ + \frac{\partial}{\partial x_i}\left(\rho \sum_{k \neq a} D_{q_k}\left(h_{v_k} - h_{v_a} \right)\frac{\partial q_{v_k}}{\partial x_i} \right) + \frac{\partial}{\partial x_i}\left(\sum_k \frac{\mu_t}{Sc_t} h_k \frac{\partial q_k}{\partial x_i} \right) \end{aligned} \tag{3}$$

$$\frac{\partial \rho q_p}{\partial t} + \frac{\partial \rho u_j q_p}{\partial x_j} = \frac{\partial}{\partial x_j}\left(\left(\rho D_p + \frac{\mu_t}{Sc_t} \right)\frac{\partial q_p}{\partial x_j} \right) \tag{4}$$

where ρ - mixture density, kg/m^3; u - velocity, m/s; P - pressure, Pa; g - gravitational acceleration, m/s^2; T - temperature, K; μ, μ_t - laminar and turbulent viscosity respectively, kg/m/s; λ, λ_t - laminar and turbulent thermal conductivity respectively, W/m/K; Sc_t - turbulent Schmidt number, dimensionless; D - molecular diffusivity, m^2/s; h - enthalpy, J/kg; q - total mass fraction (vapor and liquid if it exists). The subscripts i and j denote the Cartesian x, y and z coordinates, index p denotes the component p, index v is for the vapor phase and index a is for air. The turbulent Schmidt number is set equal to 0.72.

For the gas properties the ideal gas assumption is used, while for the liquid properties specific correlations are used. For the phase distribution the Raoult's law for ideal mixture is employed using the Rachford-Rice methodology. The liquid phase of hydrogen is assumed to be dispersed in the vapour mixture. For more details please advise Giannissi and Venetsanos, 2018 [13]. Heat convection from the ground to the cloud was modeled by solving the 1D temperature equation inside the underground.

To model the release and match the measured mass flow rate shown in Figure 1 transient conditions were imposed at the source. It was assumed that until steady state was reached the flow at the nozzle is two-phase and during steady state only liquid hydrogen is released. Thus, time-dependent functions were set in both the velocity and the vapor volume fraction. In the velocity transient function the value zero was set until 6 sec. Then, the velocity linearly increases until about 14 sec to its final steady value u=33.31 m/s. To model the initial increasing measured mass flow rate, the vapor volume fraction was decreased from α_v=1 at t=0 sec to α_v=0 at t=50 sec. The intermediate values of the vapor fraction are arbitrary chosen so as the profile to match the experimental one (see Figure 1).

As far as the numerical parameters is concerned higher order scheme (MUSCL) was used for the convective terms in all conservation equations, including that of the turbulent kinetic energy and dissipation rate. For the diffusive terms the central differences were used and for time integration the 1st order upwind scheme was applied. Low under-relaxation factor were used in all variables to promote convergence.

For the wind modeling a 1D problem was initially solved with boundary conditions on the top plane such to predict velocity equal to 2.7 m/s at 1.5 m height (following the near-field measurements). The values obtained from the 1D problem were set as inflow boundary conditions in the 3D dispersion problem. The wind was assumed aligned with the jet.

The domain of the 3D dispersion problem was extended 2 m upwind and 20 m downwind the release along x-axis, 10 m in each direction of the y-axis and 6 m was the height. No symmetry was assumed, in order to use the exact same grid with the simulation that the offset from jet release centerline wind direction is applied, which is planned for the future. One cell was used to discretize the source area and small expansion ratios up to 1.12 were used. The total number of cells was 325 526. A finer grid with 664 224 cells was also tested to check the grid independence. The results were very similar with the coarse grid results for the majority of the sensors.

4.0 RESULTS AND DISCUSSION

Due to the wind intermittency it is difficult to compare the experimental time series with the predicted ones. Thus, we consider that the peak measured concentrations in the sensors along the release plane are achieved when the wind is aligned with the release. The same stands for the minimum measured temperature. These measured values are compared with the steady state predictions. This approach has been also used in previous studies facing similar issues [10], [14].

The comparison with experiment for the near-field sensors (until 6 m from the release point) is shown in Figure 2. Both simulations are within factor of 2 for most of the sensors in terms of peak concentration and temperature. The jet centerline sensors (z=0.5 m) closer to the release point are in

good agreement with the experiment for both simulations, while they diverge from the experimental data at longer distances. There is a tendency of over prediction of the concentration and under prediction of temperature at distances longer than 2.67 m. This can be partly explained by the fluctuation of the wind direction. The peak concentration is an indication of the steady state concentration in case that the wind direction was constant and aligned with the release. However, due to wind variability greater level of mixing occurs in the experiments leading to lower concentrating levels at the sensors.

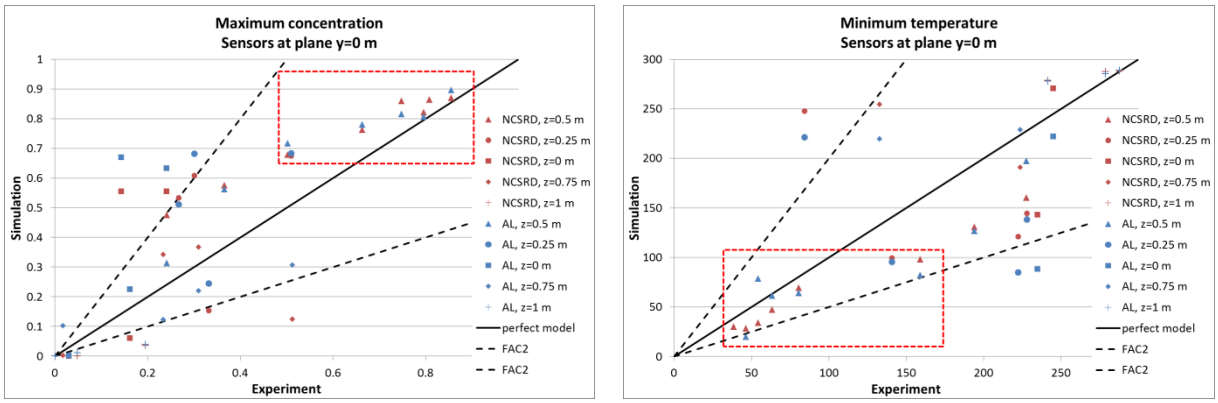

Figure 2. The predicted versus the observed peak concentration and minimum temperature on plane y=0 for all near-field sensors. The red box indicates the centreline sensors located close to the nozzle (up to 2.67 m distance).

At the highest sensors (1 m) both simulations underestimate the concentration at all distances. At the majority of the lower sensors (below the release centerline) the concentration is overestimated by both simulations with AL to give higher over-prediction. This behavior indicates that the simulations predict a lower level of buoyancy compared to the experiment.

Figure 3 shows the concentration (by volume) contour plots on release plane for the two simulations. AL predicts higher concentration levels (red area) in a region close to the ground, while NCSRD predicts a wider cloud further downwind the release. Moreover, the flammable mixture in NCSRD simulation seems to rise from the ground at closer distance than in AL simulation. The reason for these discrepancies might be the fact that AL did not model the heat convection from the ground and thus predicted a less buoyant cloud.

At this point it should be reminded that the release point in AL simulations is located at the position where hydrogen is fully vaporized (see Section 3.1), i.e. at 0.766 m according to the calculations performed with FLASH utility program. Interestingly, NCSRD CFD calculations predict that the liquid hydrogen mass fraction at 0.766 m distance from the nozzle is $3 \cdot 10^{-3}$, i.e. close to zero, while zero value is predicted after 0.83 m. Moreover, no rainout was predicted by the CFD modeling similar to FLASH utility program and the experiment.

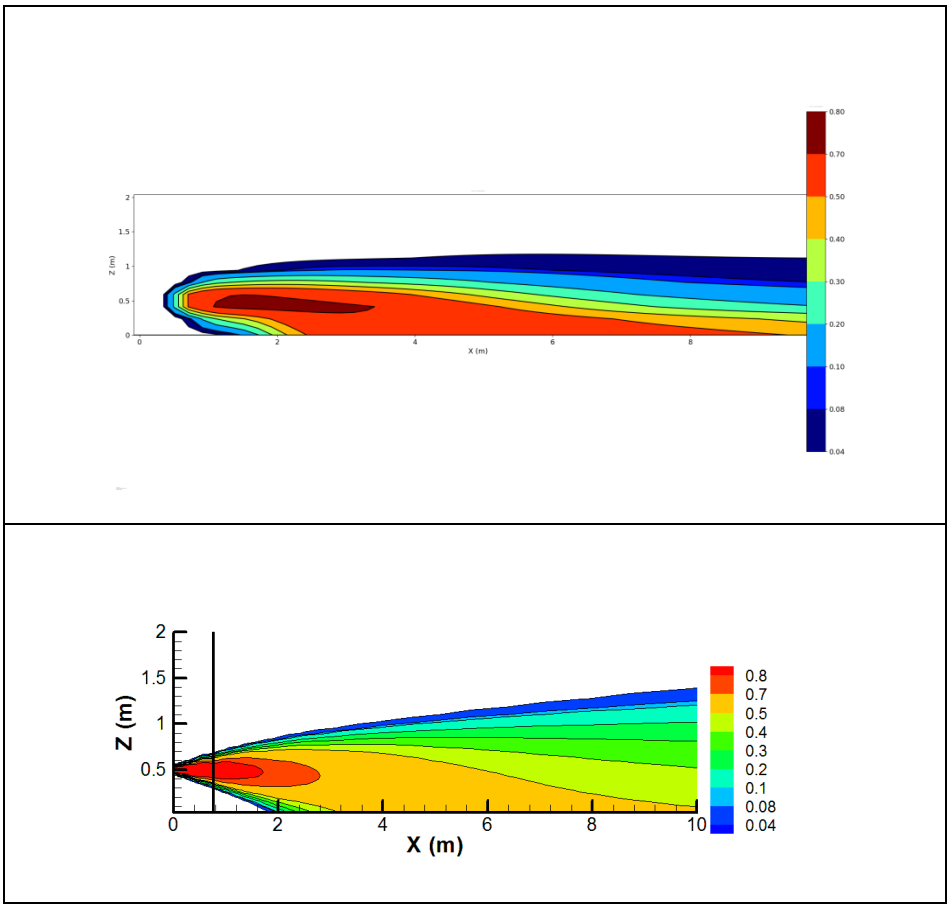

Figure 3. Concentration (by volume) contour plots for AL (top) and NCSRD (bottom) simulations. The vertical black line in NCSRD plot corresponds to the release position of AL simulation.

Figure 4 is a snapshot from the experimental video at around 35 sec, when concentration peak occurs at the closest sensor (0.35 m from release) among the jet centerline sensors. Based on the Figure at that moment the wind direction should be almost aligned with the release centerline, and, consequently, the cloud is also in line with the centerline sensors. The visible cloud during the experiment is actually the condensed ambient humidity and has a temperature equal to the dew temperature. The edge of the visible cloud corresponds to 8% hydrogen concentration [15]. For consistent comparison of the simulation results with the field measurements we produced the predicted temperature iso-surfaces that correspond to the dew point. The dew temperature, T_d, is derived by [16],

$$T_d = T - \left((100 - RH) / 5 \right) \tag{5}$$

where T is in degree Celsius and RH is ambient relative humidity in percent. This equation is fairly accurate for RH>50 %. Using the experimental ambient data (T=15.7^{o}C and RH=54.3%) eq. (5) gives a dew temperature equal to approximately 6^{o}C. The 6^{o}C temperature iso-surfaces are illustrated in Figure 4. The plots indicate that the cloud is extended beyond the far-field sensors similar to the experiment. However, in the experiment a wider spreading along the height is observed compared to predictions (see close side view). Further investigation of the level of turbulent diffusion in cryogenic releases should be considered. Moreover, the experimental cloud seems more buoyant. This can be attributed to the air components and humidity freezing, which was not modeled. In the future, simulations which will account such phenomena will be performed.

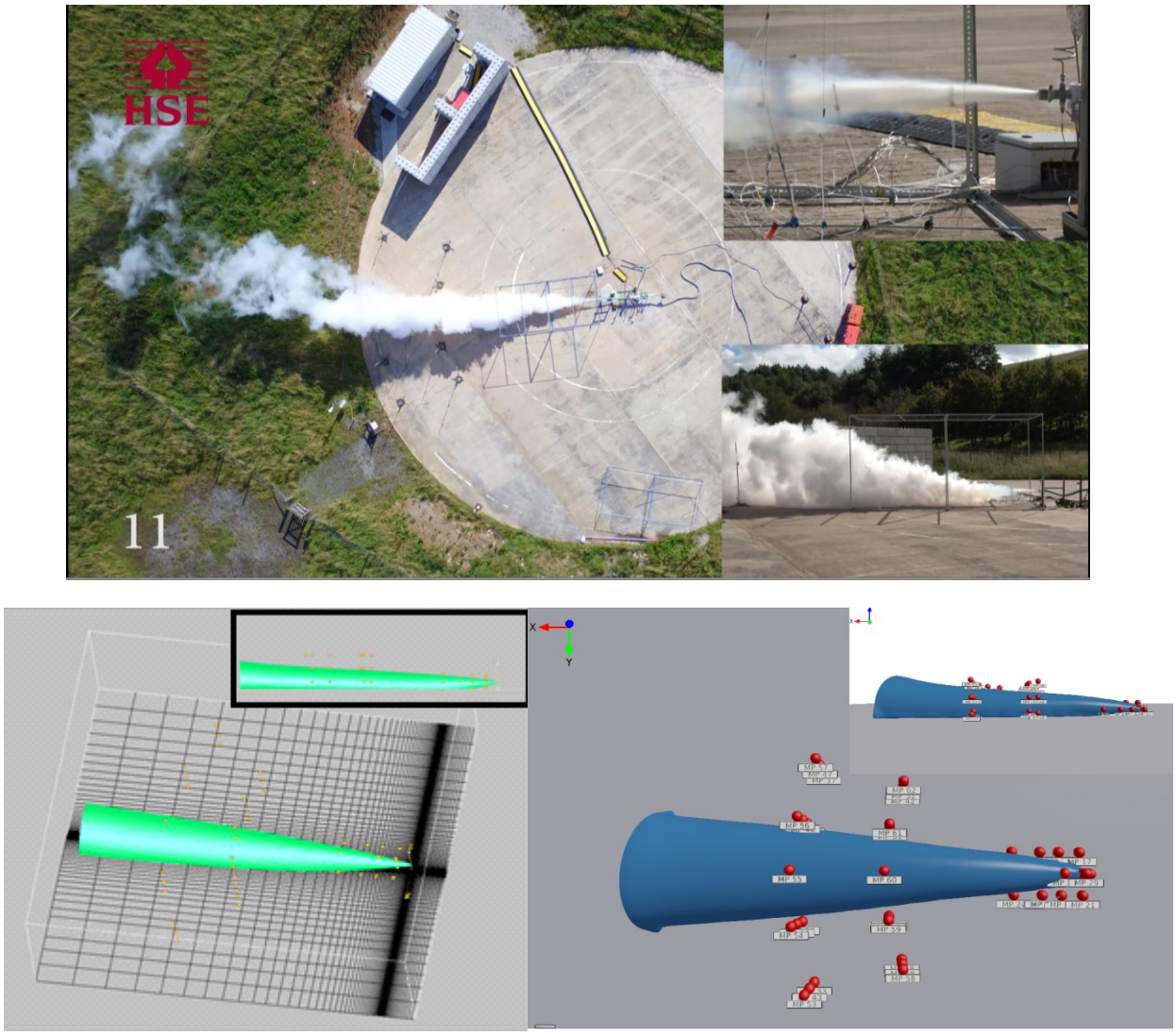

Figure 4. Snapshot from experimental video (top) at around 35 sec (top view, side view and close side view). Predicted iso-surface of dew point for NCSRD simulation (left) and for AL simulation (right).

Figure 5 is a snapshot from the experimental video at around 2.5 min, when the wind direction is offset the release centerline. The effect of wind direction on mixture dispersion is evident. The visible cloud, which more or less represents the flammable cloud, shifts away from the release centerline even at distances close to nozzle (~ 3m). This underlines the difficulty to accurately predict the concentration not only in the far-field, but also in the near-field sensors. The need to model the transient wind direction is revealed. In the past, Giannissi et al. [10] performed simulations with transient wind direction in similar experiments showing its importance. However, in the current experiment the time series of wind direction are not available with high frequency, in order to be exploited.

Figure 5. Snapshot from experimental video at around 2.5 min (top view, side view and close side view).

5.0 CONCLUSIONS

An inter-comparison between simulations and experiment has been carried out and presented here. The work has been performed within the PRESLHY project. Two partners, Air Liquide (AL) and National Center for Scientific Research "Demokritos" (NCSRD), simulated experiments performed by the Health and Safety Executive (HSE) that involved liquid hydrogen release in open environment. The release was horizontal 0.5 m above concrete ground through a 12 mm nozzle. The steady state mass flow rate was 265 g/s. Based on the experimental data no flashing occurs at the nozzle and thus only liquid release is established.

AL assumes only vapor phase in the dispersion simulations. It uses the FLASH utility program to calculate an equivalent source area where all liquid has been evaporated. This equivalent source is set as input in the CFD simulation and is located 0.766 m downstream the real nozzle. On the contrary, in NCSRD simulation pure liquid is released at the time when experimentally steady state mass flow rate is achieved and it solves for the resulting two-phase mixture (liquid and vapor hydrogen) in the CFD domain. Interestingly, the two-phase flow modeling approach of NCSRD predicted an almost zero mass fraction of liquid (10^{-3} magnitude of order) at the same distance from the nozzle as FLASH utility program calculated. Moreover, no rainout was predicted by both CFD modeling and the FLASH program similar to what was observed in the experiments.

Both simulations assume wind direction in line with the release, while in experiment the wind direction exhibited high fluctuations. Due to the wind intermittency the comparison among the predictions and the experiment is performed only for the near-field sensors. For the comparison it is assumed that the experimental peak is achieved when the wind is aligned with the release as assumed in simulations. Therefore, the experimental peak concentration and minimum temperature are compared with the steady state predicted concentration and temperature. This practice has been applied in the past in other studies as well.

The comparison demonstrated that both simulations are within factor of 2 for most of the sensors in terms of concentration and temperature predictions. The jet centerline sensors (z=0.5 m) are in good agreement with the experiment for both simulations. However, the computational results are closer to the field measurements near to the release point, whereas the tendency to diverge from the experimental data (over-prediction) is observed at longer distances. This can be partially explained by

the fluctuation of the wind direction. At the highest sensors simulations under-predict the concentration, while at the sensors lower than the release centerline the concentration is over-predicted.

Finally, NCSRD predicted more buoyant cloud than AL most likely because AL neglected the heat convection from the ground to the cloud. Yet, in the experiments the visible cloud seems to be lifted even more. Other factors, such as humidity and air component condensation, could have contributed to the total heat input that the cloud received and became more buoyant. In the future, simulations that take into account all heat sources to the cloud will be conducted.

6.0 ACKNOWLEDGMENTS

The research leading to these results was financially supported by the PRESLHY project, which has received funding from the Fuel Cells and Hydrogen 2 Joint Undertaking under grant agreement No 779613. This Joint Undertaking receives support from the European Union's Horizon 2020 research and innovation programme, Hydrogen Europe and Hydrogen Europe research.

The HSE work programme acknowledges funding from its sponsors Shell, Lloyd's Register Foundation and Equinor and instrumentation provided by NREL and Dräger.

REFERENCES

[1] PRESLHY, "https://preslhy.eu/," *Pre-normative REsearch for Safe use of Liquid HYdrogen, esearch and Innovation Action Supported by the FCH JU – Grant Agreement No 779613*, 2017. .

[2] J. Hall *et al.*, "HSE SD experimental summary for the characterisation, dispersion and electrostatic hazards of LH2 for the PRESLHY project," in *International Conference on Hydrogen Safety, Edinburgh, UK, September 21-23*, 2021.

[3] G. A. Number, S. Jallais, and L. Bernard, "D3.6 Summary of experiments series E3.5 (Rainout) results," *Rep. PRESLHY Proj.*, no. May, 2018.

[4] FLACS, "FLACS-CFD V20.1, User's Manual, Bergen, Norway," 2020.

[5] B. E. Launder and D. B. Spalding, "The numerical computation of turbulent flow," *J. Comput Methods Appl Mech Eng*, vol. 3(2), pp. 269–289, 1974.

[6] H.-C. Salvesen, "Modelling of jet release of liquefied gas under high pressure. Report Christian Michelsen Research, CMR-95-F20062 (Confidential).," 1995.

[7] A. M. Monin, A. S. & Obukhov, "Basic laws of turbulent mixing in the surface layer of the atmosphere.," *Tr. Akad. Nauk SSSR Geofiz. Inst*, vol. 24, pp. 163–187, 1954.

[8] R. A. P. M. Bosch, C. J. H. van den & Weterings, "Methods for the calculation of physical effects. Report TNO CPR14E.," 1996.

[9] S. G. Giannissi, A. G. Venetsanos, N. Markatos, and J. G. Bartzis, "Numerical simulation of LNG dispersion under two-phase release conditions," *J. Loss Prev. Process Ind.*, vol. 26, no. 1, pp. 245–254, Jan. 2013.

[10] S. G. Giannissi, A. G. Venetsanos, N. Markatos, and J. G. Bartzis, "CFD modeling of hydrogen dispersion under cryogenic release conditions," *Int. J. Hydrogen Energy*, vol. 39, no. 28, pp. 15851–15863, Sep. 2014.

[11] S. G. Giannissi, "CFD modeling of hydrogen and natural gas dispersion, Doctoral Dissertation, National Technical School of Athens, http://hdl.handle.net/10442/hedi/39339," 2016.

[12] A. Venetsanos and J. Bartzis, "CFD modeling of large-scale LH2 spills in open environment," *Int. J. Hydrogen Energy*, vol. 32, no. 13, pp. 2171–2177, Sep. 2007.

[13] S. G. Giannissi and A. G. Venetsanos, "Study of key parameters in modeling liquid hydrogen release and dispersion in open environment," *Int. J. Hydrogen Energy*, vol. 43, no. 1, pp. 455–467, 2018.

[14] M. Ichard, O. R. Hansen, P. Middha, and D. Willoughby, "CFD computations of liquid hydrogen releases," *Int. J. Hydrogen Energy*, vol. 37, no. 22, pp. 17380–17389, Nov. 2012.

[15] J. Witcofski, RD, Chirivella, "Experimental and analytical analyses of the mechanisms

governing the dispersion of flammable clouds formed by liquid hydrogen spills," *Int. J. Hydrogen Energy*, vol. 9, no. 5, pp. 425–435, 1984.

[16] M. G. Lawrence, "The relationship between relative humidity and dewpoint temperaure in moist air: A simpe conversion and applications," *Bull. Amer. Meteor. Soc.*, vol. 86, pp. 225–233, 2005.